Speech-driven 3D Facial Animation with Implicit Emotional Awareness: A Deep Learning Approach

Hai X. Pham[1], Samuel Cheung[2], and Vladimir Pavlovic[1]

[1]Department of Computer Science , Rutgers University
{*hxp1,vladimir*}*@cs.rutgers.edu*
[2]Department of Electrical and Computer Engineering , Rutgers University
sc1528@rutgers.edu

Abstract

We introduce a long short-term memory recurrent neural network (LSTM-RNN) approach for real-time facial animation, which automatically estimates head rotation and facial action unit activations of a speaker from just her speech. Specifically, the time-varying contextual non-linear mapping between audio stream and visual facial movements is realized by training a LSTM neural network on a large audio-visual data corpus. In this work, we extract a set of acoustic features from input audio, including Mel-scaled spectrogram, Mel frequency cepstral coefficients and chromagram that can effectively represent both contextual progression and emotional intensity of the speech. Output facial movements are characterized by 3D rotation and blending expression weights of a blendshape model, which can be used directly for animation. Thus, even though our model does not explicitly predict the affective states of the target speaker, her emotional manifestation is recreated via expression weights of the face model. Experiments on an evaluation dataset of different speakers across a wide range of affective states demonstrate promising results of our approach in real-time speech-driven facial animation.

1. Introduction

Human-machine interaction has been one active research area for decades, with the ultimate goal to make human-machine interaction transparent. Speech, as a natural form of communication among various modes of interactions, is becoming more immersive, evidenced by the increasing popularity of virtual voice assistants, such as Microsoft's Cortana or Amazon's Alexa, in our daily lives. Furthermore, not only the contextual sound units (phonemes) are carried in the audio recording, but also emotional states of the speaker via speed or intensity of her speech [18, 6, 4, 17, 5]. Thus, a lively animated 3D head representing the speaker will certainly enhance the speech perception experience in many applications. One such application is the development of talking agent, either in the form of virtual or physical (i.e. robotic) avatars, for face-to-face human-machine interaction, as in computer-assisted voice agent. In this scenario, the recorded speech can easily be manipulated, by changing the speed or pitch, to reflect the artificial emotion of the digital assistant. These changes can be automatically reflected visually on the avatar, and make the interaction more engaging. On the other hand, it can also make inter-person telecommunication more enjoyable by expressing speech via personalized avatars, especially in interactive role-playing games, where the gamers communicate with other characters in the virtual world.

In this work, we aim to recreate a talking 3D virtual avatar that can naturally rotate and make micro facial movements to reflect the time-varying contextual information and emotional intensity carried in the input speech. Intuitively, this work is analogous to visual 3D face tracking [20, 19], however, it is more challenging as we try to map acoustic sequence to visual space, instead of conveniently relying on textural cues from input images. Moreover, speech-emanating facial movements involve different activations of correlated regions on the geometric surface, thus it is difficult to achieve realistic looking, emotion-aware facial deformation from speech sequence.

Thus, we propose a regression framework based on long short-term memory recurrent neural network to estimate rotation and activation parameters of a 3D blendshape face model [7] from sequence of acoustic features, for real-time life-like facial animation. We extract a wide range of acoustics features to capture contextual and emotional progression of the speech. To tackle the difficulty of avatar gen-

eration, we utilize the blendshape model in [7], which is purposely designed with enough constraints to ensure that, the final model would always look realistic given a specific set of control parameters. In addition, it can represent various emotional states, e.g. sadness, happiness, etc., without explicitly specifying them. In order to directly map the input features to face shape parameters, we use deep recurrent neural network with LSTM cells [15] to model the long range context of the sequence.

2. Related Work

Text or speech-driven facial animation. Usually related in the literature as "talking head", various approaches have been developed to animate a face model driven by either text or speech. A text-driven approach typically consists of a text-to-speech and a text-to-face shape synthesizing unit, and are combined to generate facial animation [24, 9]. Speech-driven techniques often share a common approach: directly map an input sequence of acoustic features to a sequence of visual features [13, 29, 22].

The above approaches can also be categorized according to the underlying face model, into model-based [2, 1, 23, 28, 10, 8] and image-based [3, 9, 12, 25, 29, 13]. Image-based approaches compose the output video by concatenating short clips, or stitch different regions from a sample database identified by a classifier, together. These approaches usually generate photo-realistic video output, as they compose the result from real images with natural textures. However, their performance and quality are limited by the amount of samples in the database, thus it is difficult to generalize to a large corpus of speeches, which would require a tremendous amount of image samples to cover all possible facial appearances. In contrast, although lacking in photo-realism, model-based approaches enjoy the flexibility of a deformable model, which is controlled by only a set of parameters, and more straightforward modeling.

Essentially, every talking head animation technique requires a particular algorithm in order to map an input to visual features, which can be formulated as a regression or classification task. Classification approaches usually identify phonetic unit (phonemes) from speech and map to visual units (visemes) based on specific rules, and animation is generated by morphing these key images. Regression approaches, on the other hand, can directly estimate visual parameters from input features and generate continuous trajectories. Early successes in speech-driven talking head were achieved by using Hidden Markov models (HMMs) for trajectory estimation [25, 26]. However, HMM-based techniques incur certain limitations of generative model, e.g. wrong model assumption, or over-smoothing because of the maximum likelihood framework. In recent years, deep neural networks have been successfully applied to speech synthesis [21, 30] and facial animation [10, 31, 13] with superior performance. This is because deep neural networks are able to learn the correlation of high-dimensional input data, and, in case of recurrent neural network, long-term relation, as well as the highly non-linear mapping between input and output features.

Long short-term memory recurrent neural networks. Recurrent neural networks (RNNs) [27] have demonstrated highly desirable performance in sequence modeling with the ability to integrate temporal contextual information. Hochreiter et al. [15] introduced the Long short-term memory (LSTM) cell in RNN to overcome the vanishing gradient problem [14] in modeling long-term relation. In this work, we aim to estimate the facial transformation trajectory in real-time, hence we utilize unidirectional (forward) LSTM-RNN that only memorizes the past data.

3. System Overview

Figure 1 illustrates the architecture of our proposed speech-driven facial animation framework, which includes a training stage and an animation stage. In the training phase, the speech-to-facial parameters mapping is learned by a LSTM-RNN model from the RAVDESS database [16], a large audio-visual corpus that consists of high resolution videos of various speeches and emotions (cf. 6 for more details). High quality videos allow accurate visual tracking of 3D facial deformations, which subsequently enable the deep model to learn complex mapping between speeches and facial actions. Our method is totally language-independent, hence it can be extended with more samples of other subjects speaking different languages. In the animation phase, the trained LSTM model converts input acoustic features into head rotation and facial deformation parameters to drive a 3D blendshape face model.

At the first step in the training phase, various input acoustic features and expected visual output, including head rotation and local deformation parameters, are extracted from training videos (cf. 4 for details on feature and parameter extraction). Subsequently, they are used to train a discriminative LSTM-RNN model by minimizing a squared loss, in order to effectively learn the non-linear mapping between input features and output parameters. The animation phase is very straightforward: given a recorded speech sequence and its features, the LSTM-RNN model estimates head rotation and deformation parameters, which are then used to animate a 3D face model to visually recreate the facial movements and expression carried in the input speech.

4. Feature Representation

4.1. Face Model Parameterization

In this work, we utilize the 3D blendshape face model from the FaceWarehouse database [7], in which, an arbitrary shape S including head pose of a subject can be com-

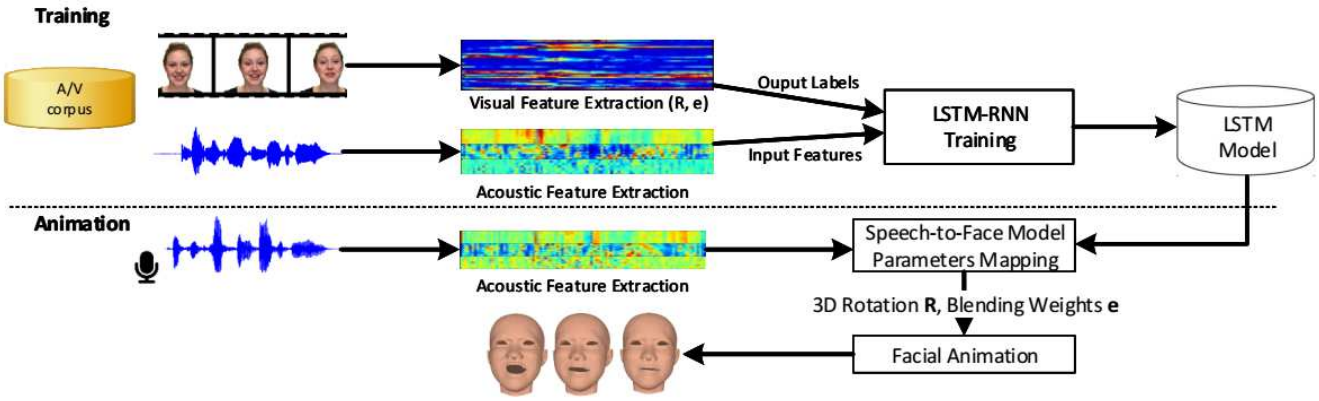

Figure 1: The proposed speech-driven facial animation framework.

posed as:

$$S = R\left(B_0 + \sum_{i=1}^{N}(B_i - B_0)e_i\right), \qquad (1)$$

where (R, e) are rotation and expression blending parameters, respectively, $\{B_i|i = 1..N\}$ are personalized expression blendshape bases of a particular person, calculated from a 3D tensor, and their combinations are consistent across users. Note that $\{e_i\}$ are constrained within $[0, 1]$. Readers are encouraged to find more details about the FaceWarehouse face model and its parameterization in [7].

Rotation and deformation parameters (R, e) are the output of our deep model, where R is represented by three free parameters of a quaternion. In our implementation, the number of expression bases N is 46, hence the output parameter vector holds 49 values in total. We use the real-time 3D face tracker in [20], using only RGB input, to extract these parameters from training videos. In particular, the face tracker recovers facial parameters in each input video frame by performing two steps: 3D face alignment and refinement. In the alignment step, 3D facial parameters are rapidly estimated by a random forest-based heterogeneous regression pipeline trained upon regular image datasets, which also predicts 2D landmarks corresponding to a set of specific 3D vertices of the blendshape model in order to account for unseen identities and expressions. In such cases, 2D displacement errors tend to be large, i.e. the predicted 2D landmarks differ from the 2D projection of their corresponding 3D vertices considerably, and these errors are minimized in the subsequent refinement step. In this step, 3D facial parameters are fine-tuned by deforming the 3D face model to fit 2D landmarks estimated by the regressor, while maintaining temporal coherency w.r.t. previous frames. Figure 2 shows a few sample frames from the RAVDESS training set.

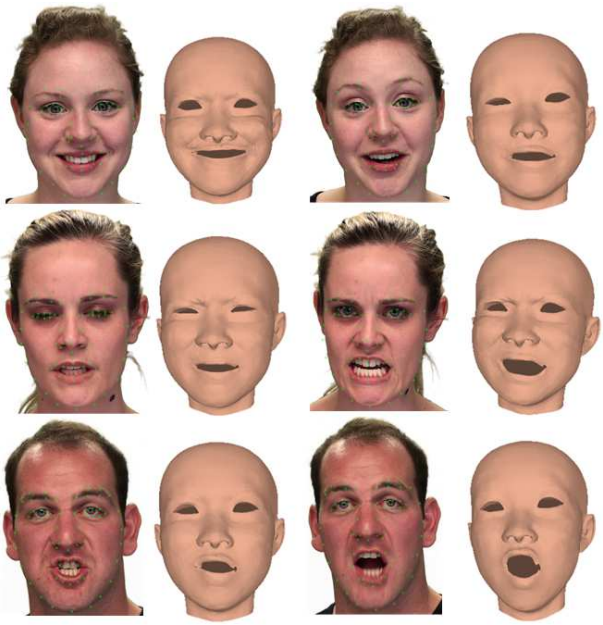

Figure 2: A few samples from the training data, where a 3D facial blendshape is aligned to the face of the actor in the input frame. Green dots mark 3D landmarks of the model projected to image plane. The blendshape rendered here is, however, a generic model animated given parameters estimated by the tracker. We also use this 3D shape model in our animation experiments.

4.2. Input Feature Extraction

The input to our system can be any arbitrary speech of any length. As we only use low-level acoustic features, our model is not tied to any particular language, and it can be easily extended given more training samples. Specifically, we extract Mel-scaled spectrogram, Mel frequency cepstral coefficients (MFCCs) and chromagram from the audio sequence. Mel-scaled spetrogram and MFCCs are standard

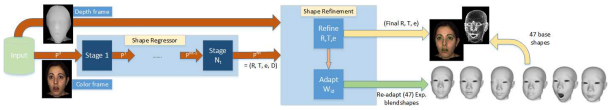

Figure 3: The tracking framework in [20], including a multi-stage regression pipeline that predicts (R, T, e), and a refinement step that fine-tunes those transformation parameters, plus identity parameters. However we do not use depth data in this work, as RAVDESS only contains regular RGB videos, and translation T and identity parameters are not used. We are only interested in estimating head rotation and facial action deformations from speech.

acoustic features proven to be very effective in presenting the contextual information, whereas chromagram is necessary to determine the pitch in the speech, which reflects the affective states of the speaker throughout the entire sequence.

We assume that every input audio sequence is synchronized to the corresponding video at 30 FPS and the audio sampling rate is at 44.1 kHz. Thus, for every video frame, there are 1,470 corresponding audio samples. We include additional samples from the previous video frame, such that for each video frame there is enough audio data to extract three windows of 25ms each, with hop length of 512 samples. In every audio window, values of 128 Mel bands, 13 Mel frequency cepstral coefficients and their delta and delta-delta coeffcients, and 12 chroma bins, are extracted. In summary, the input feature vector for every video frame has 537 dimensions, and each variable is normalized to zero mean - unit variance. Figure 4 illustrates different feature sequences extracted from videos of the same actor speaking the same sentence in different emotional states.

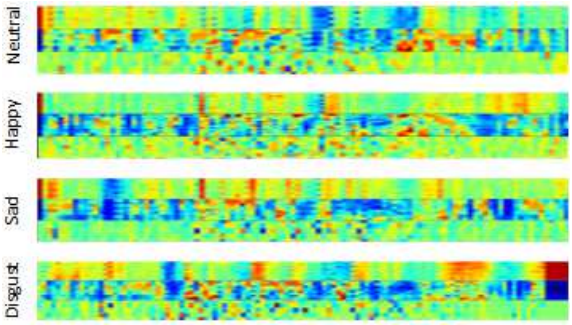

Figure 4: Feature sequences extracted from videos of the same actor speaking the same sentence "*Kids are talking by the door*" under different emotional states. From top row: Neutral, Happy, Sad and Disgust, respectively.

5. Deep LSTM-RNN for Facial Animation

5.1. LSTM-RNN

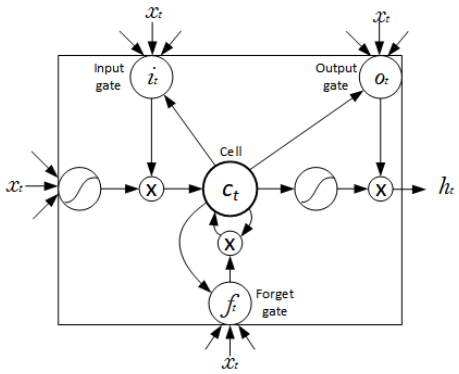

Figure 5: A long short-term memory block.

Recurrent neural networks (RNNs) have the ability to memorize past inputs in internal states. They are able to incorporate temporal contextual information, thus RNNs are very suitable for sequence modeling. However, conventional RNNs can only remember limited range of past context because of the vanishing gradient problem [14]. Long short-term memory (LSTM) unit, shown in Figure 5, is designed to overcome this limitation. LSTM unit is able to store its value for long period of time by controlling the flow of information into and out of its memory. A forward pass in the recurrent hidden layer of LSTM-RNN is as follows:

$$
\begin{aligned}
i_t &= \sigma\left(W_{xi}x_t + W_{hi}h_{t-1} + W_{ci}c_{t-1} + b_i\right), \\
f_t &= \sigma\left(W_{xf}x_t + W_{hf}h_{t-1} + W_{ci}c_{t-1} + b_f\right), \\
a_t &= \tau\left(W_{xc}x_t + W_{hc}h_{t-1} + b_c\right), \\
c_t &= f_t c_{t-1} + i_t a_t, \\
o_t &= \sigma\left(W_{xo}x_t + W_{ho}h_{t-1} + W_{co}c_t + b_o\right), \\
h_t &= o_t \tau(c_t), \\
y_t &= \eta\left(W_{hy}h_t + b_y\right),
\end{aligned}
\tag{2}
$$

where σ and τ are *sigmoid* and *tanh* activation functions, i, o, f, a and c are input gate, output gate, forget gate, cell input activation and cell memory, respectively. $t = 1..T$, where T is the sequence length. x_t is the input at time t, while h_t is the output of the hidden layer, y_t is the final output of the network, and η is the activation function of the output layer. $\{W\}$ and $\{b\}$ are weight matrices and bias vectors, respectively.

5.2. LSTM-RNN for Facial Action and Rotation Synthesis

Our framework maps input acoustic feature vector sequence of $x_t, t = 1..T$ to output sequence of shape parameter vectors y_t, where T is the number of video frames. Thus, at any given time t, the deep LSTM model estimates $y_t = (R_t, e_t)$ from an input feature vector x_t. Blending

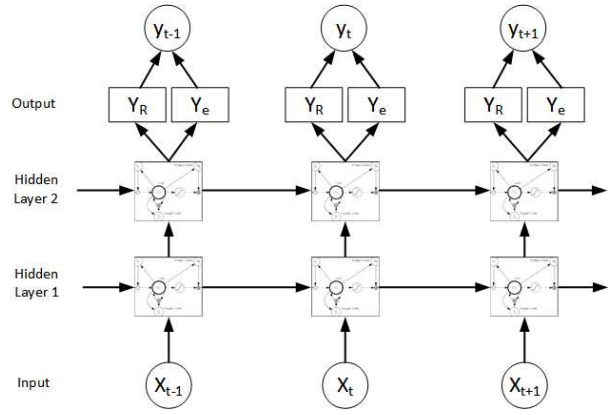

Figure 6: The architecture of our deep LSTM-RNN model for facial action and rotation synthesis. In this figure we only show two hidden layers, which we empirically found to perform reasonably well on the RAVDESS dataset.

weights e_t in particular have to be constrained within $[0, 1]$, hence we split the output into two separate layers, Y_R for rotation and Y_e for expression weights. Y_R is simply a linear layer, whereas Y_e uses ReLU activation to enforce non-negativity on the output:

$$\begin{aligned} y_{Rt} &= W_{hy_R} h_t + b_{y_R}, \\ y_{et} &= ReLU\left(W_{hy_e} h_t + b_{y_e}\right), \\ y_t &= \left(y_{Rt}, y_{et}\right). \end{aligned} \tag{3}$$

The architecture of our deep LSTM-RNN model is illustrated in Figure 6. We train the model by minimizing the square error:

$$E = \sum_t \left\| y_t - \widehat{y}_t \right\|^2, \tag{4}$$

where $\hat{y}_t$ is the expected output, which we extract from training videos.

6. Experiments

Dataset. We use the Ryerson Audio-Visual Database of Emotional Speech and Song (RAVDESS) [16] for training and evaluation. Specifically, the database consists of 24 professional actors (12 male and 12 female, respectively) speaking and singing with various emotions. The speech set consists of eight general emotional expressions: neutral, calm, happy, sad, angry, fearful, surprise, and disgust, where each video sequence is associated with one among eight affective states. Similarly, the song set, in which the actors sing short sentences, consists of six general emotional expressions: neutral, calm, happy, sad, angry, and fearful. Both sets are used for training and testing. We use video sequences of the first 20 actors for training, with around 250,000 frames in total, and evaluate the model on the data of four remaining actors.

Implementation Details. Our framework[1] is implemented in Python, based on the deep learning toolkit CNTK[2]. We train the deep models in 300 epochs, where learning rate is chosen as 0.003 for the first two epochs, 0.0015 for the next 12, and 0.0003 for the remaining epochs. Excluding the time for acoustic feature extraction, it takes about 5ms on average to estimate output vector y_t from one input frame x_t, on a laptop equipped with a relatively low-end Quadro K1000M GPU. Thus, our model is suitable for real-time speech-driven animation task.

Evaluations. We train and evaluate performance of three different LSTM-RNN topologies, as listed in Table 1, in which we also compare their performance with support vector regression (SVR) [11]. The metrics in this table is mean squared error of parameters over all video frames in the held-out test set:

$$\varepsilon = \frac{1}{M} \sum_{i=1}^{M} \left\| y_i - \widehat{y}_i \right\|^2,$$

where M is the number of video frames, y and $\hat{y}$ are model and expected output, respectively. According to this table, all deep models outperform the SVR baseline, and **Net 1** achieves the smallest training error after 300 epochs, but its testing error is slightly higher than other two network models across all affective states in the database. Moreover, we use the speech model-generated parameters and tester-specific blendshape expression units estimated by the visual tracker to calculate a person-specific 3D shape as in (1), and extract its landmarks in order to compare to visual tracking results. In particular, Table 2 and 3 contain root mean squared error (RMSE) of 3D landmarks in millimeters and RMSE of projected 2D landmarks normalized over average head size, which equals to 400 pixels in RAVDESS, respectively. Figure 8 shows histogram of landmark errors of a few key landmarks.

According to Table 2, the average 3D error of deep models is about 10mm. It is expected because speech-driven models cannot accurately estimate head rotation. Specifically, each actor has a different person-specific rigid head movement pattern, whereas the deep models learn to estimate head rotation by averaging over all training samples as in (4). Thus, these models are unable to effectively reproduce accurate rigid head movement on the test data. However, rigid rotations, temporally smoothed by RNN, can augment the 3D animation for more realistic visual effect, compared to a stationary head. In general, in terms of shape error, all three network models achieve similar errors, with **Net 3** slightly outperforms the other two, but the difference in 3D error is less than 1mm. These results demonstrate that our deep models can generate consistently realistic 3D

[1] Code available at: research.cs.rutgers.edu/∼hxp1/SpeechProject.html
[2] Microsoft Cognitive Toolkit (cntk.ai)

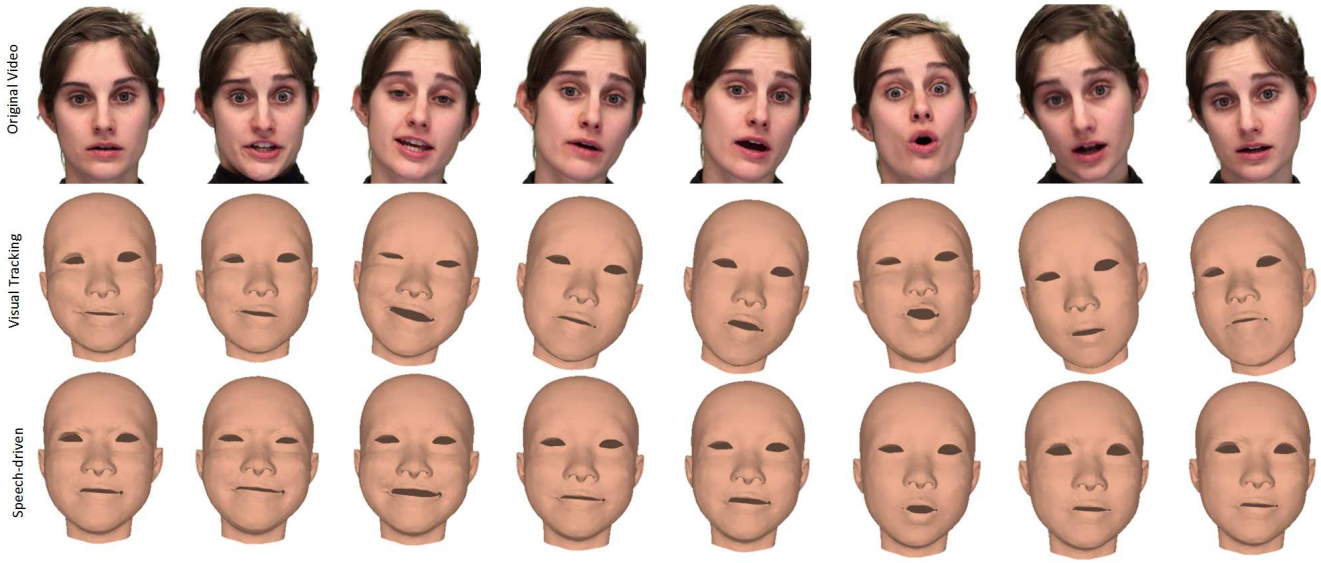

(a) Actor 24 - Surprised

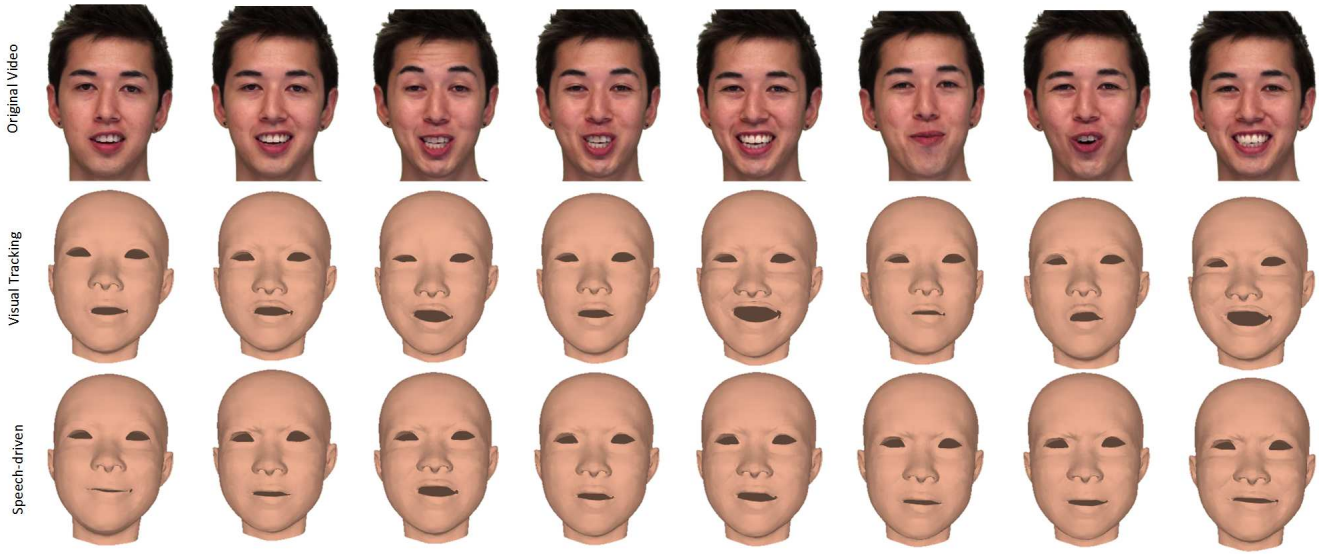

(b) Actor 21 - Happy

Figure 7: Two sequences from the test set. For each sequence, shown from top to bottom: the original video, the 3D blendshape animated by the visual tracker [20] and the speech-driven animation generated by our deep model, respectively.

Table 1: Training and testing errors of different network configurations. For example, 1:600-2:200 means this is a 2-hidden-layer LSTM-RNN whose 1^{st} and 2^{nd} hidden layers have 600 and 200 units, respectively. Testing error is also separated corresponding to eight affective states, e.g. the "Happy" column contains mean squared error over all frames in videos labeled with "happy" general emotion.

	Configuration	**Train. Err.**	**Test Err.**	*Neutral*	*Calm*	*Happy*	*Sad*	*Angry*	*Fear*	*Disgust*	*Surprised*
Net 1	1:600-2:200	**0.59**	**3.22**	3.22	3.26	3.44	3.27	2.96	3.06	3.53	3.17
Net 2	1:300-2:200	**1.08**	**3.03**	2.98	2.98	3.25	3.09	2.81	2.89	3.30	3.10
Net 3	1:600-2:600	**0.79**	**3.06**	3.02	3.14	3.37	3.10	2.69	2.94	3.30	3.02
SVR	n/a	**3.39**	**3.50**	3.52	3.40	3.84	3.45	3.32	3.34	3.62	3.70

Table 2: RMSE (in mm) when comparing reconstructed 3D landmarks using the speech model-generated parameters to visual tracking results. **Net 3** achieves smaller error overall.

	Overall	Neutral	Calm	Happy	Sad	Angry	Fear	Disgust	Surprised
Net 1	**10.11**	9.15	9.87	9.31	10.89	9.19	10.70	12.70	8.99
Net 2	**10.58**	9.47	10.61	9.50	11.18	9.56	10.98	13.67	9.95
Net 3	**9.91**	8.60	9.90	8.96	10.68	8.84	10.60	12.39	9.04
SVR	**20.30**	21.55	30.33	20.62	19.88	18.82	19.63	23.06	20.65

Table 3: Normalized RMSE when comparing reconstructed 2D landmarks using the speech model-generated parameters to visual tracking results. 2D landmarks are created by projecting 3D corresponding landmarks onto the image plane.

	Overall	Neutral	Calm	Happy	Sad	Angry	Fear	Disgust	Surprised
Net 1	**0.050**	0.041	0.048	0.045	0.055	0.045	0.053	0.063	0.044
Net 2	**0.053**	0.045	0.054	0.047	0.056	0.047	0.054	0.070	0.050
Net 3	**0.050**	0.040	0.050	0.044	0.054	0.044	0.053	0.063	0.045
SVR	**0.070**	0.064	0.073	0.066	0.073	0.066	0.073	0.079	0.067

facial animation, despite the limitation in rigid motion estimation, thanks to the underlying blendshape model. However, a thorough user study is desirable in order to measure the quality of animation generated by these models, which we look forwards to conducting in the future.

From our visual observation, **Net 1** consistently outperforms other networks, in terms of local facial deformation quality, especially in lower lip movements, indicated by smaller landmark error as shown in Figure 8. In order to explain this phenomenon, we further categorize estimation errors into separate bins for individual blending weights e_i for each network, as shown in Figure 9.

According to this figure, **Net 2** and **Net 3** have very similar errors across all coefficients with the exception of units 20 and 24, whereas **Net 1** has higher errors with expression units 7, 8, 32 and 46. However, these units carry very subtle facial deformations, and thus do not affect the face reconstruction quality of **Net 1** in general. A possible explanation is that, **Net 2** and **Net 3** tend to smooth output parameters to achieve lower mean error, trading off the ability to model spontaneity of facial expressions. Further investigation is needed in order to understand how the unbalanced architecture of **Net 1** contributes to this phenomenon. Figure 10 demonstrates that **Net 1** achieves smallest errors on the parameters most relevant to the "Surprised" state of Actor 24.

Figure 7 shows two example sequences from the test set. Both actors speak the same sentence, *"Kids are talking by the door"*, but under different emotions, tones and speeds. Facial parameters are estimated by **Net 1**. Speech-driven animation quality on the first sequence from Actor 24 is rather good, where micro facial movements estimated by our model match closely to that of the visual tracker [20]. However, our model cannot effectively recreate lip deformations in the "Happy" sequence of Actor 21.

Poor estimation performance on "happy" sequences in general, as shown in Table 1, can be accounted for by a couple of reasons. First, the amount of "happy" frames is only one seventh of the entire dataset. It causes bias of the model towards more similar emotions, such as "angry", "fearful" and "disgust". Second, it is difficult to distinguish the "happy" speech from "surprised" or "angry" from speech alone as under these emotions, speakers tend to speak equally loudly. Lastly, although smiling is a very strong visual cue, it is not reflected via speech in an obvious way. Note that in these "happy" sequences, the actors do not actually laugh at any time, but rather smile while speaking, hence it is difficult to recognize the smiling gesture from speech. More analysis on "happy" speeches is required in order to identify the smiling cue from audio data.

7. Conclusion and Future Work

This paper presents a deep recurrent learning approach for speech-driven 3D facial animation. Our regression framework, based on deep long short-term memory recurrent neural network, directly maps various acoustic features of an input speech sequence to head rotation and facial deformation parameters of a 3D blendshape model for realistic animation in real-time. Experimental results on a real audio-visual corpus consisting of speeches under various emotions demonstrate the effectiveness of our approach in recreating the affective state and facial deformation of the speaker. We believe our work is a reasonably good baseline for further research in speech-driven facial animation. In the future, we will explore the ability to learn features directly from the raw waveform data, and incorporate deep generative model in our framework to improve its facial parameter generation quality.

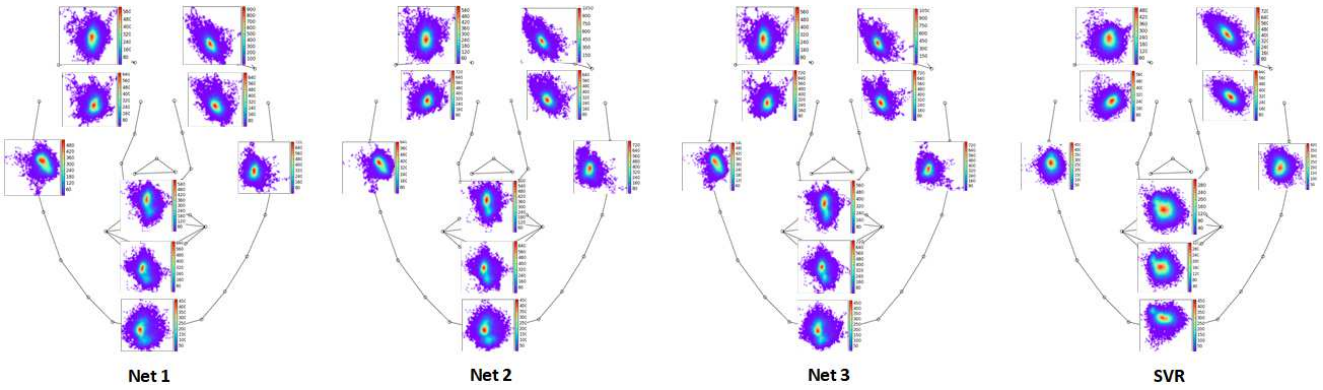

Figure 8: Histograms of landmark error distributions corresponding to eyebrows, upper eyelids, chin, cheeks, upper lip and lower lip. Data points in bins closer to the center of the histogram have smaller errors.

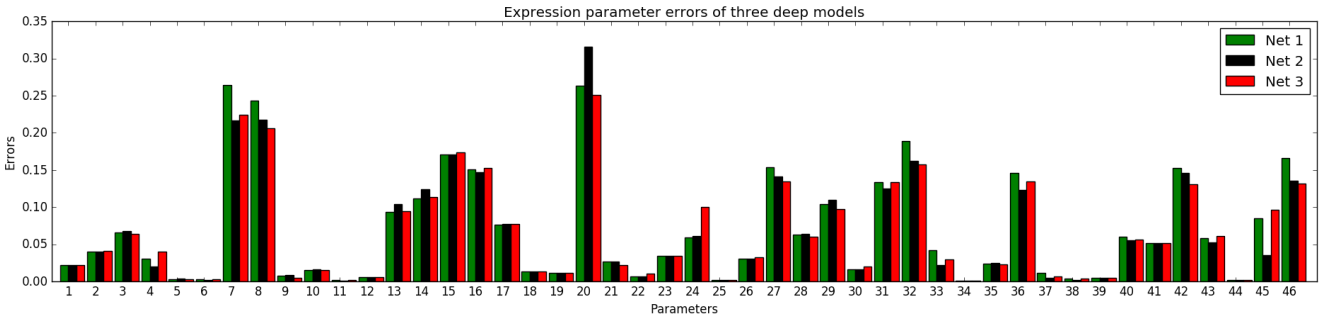

Figure 9: Parameters errors of three LSTM models, categorized by expression units.

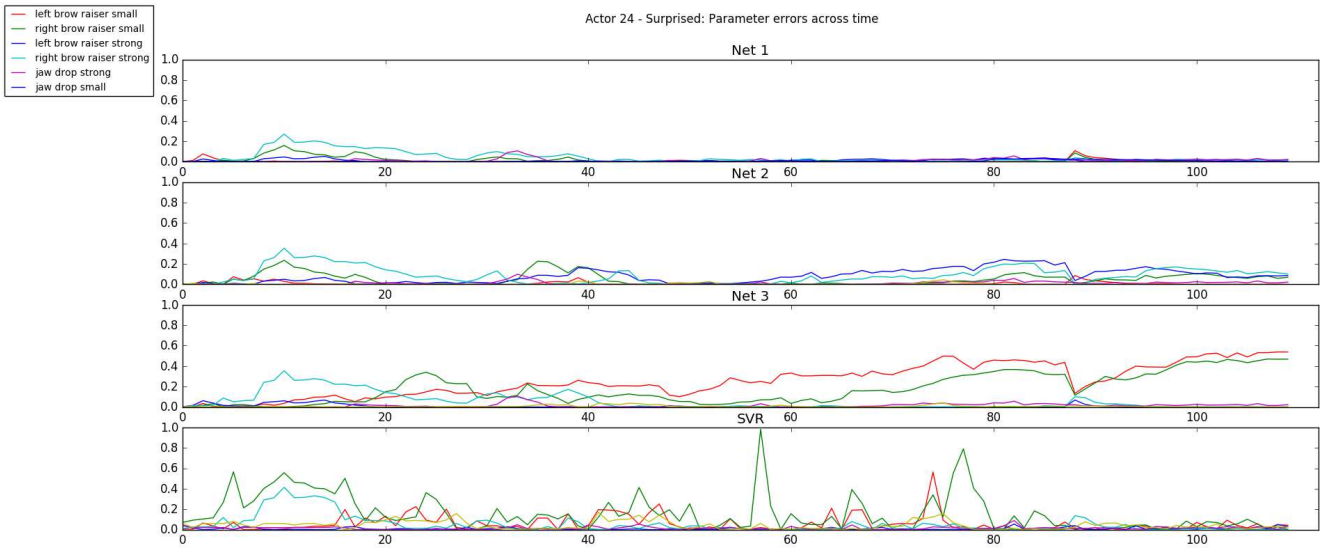

Figure 10: Parameter errors across time of the "Actor 24 - Surprised" sequence. We plot errors corresponding to six action units: left/right eyebrow raiser small/strong and jaw dropper small/strong. From top to bottom: plots of of **Net 1**, **Net 2**, **Net 3** and **SVR**, respectively. **Net 1** achieves smallest errors w.r.t. these action unit parameters. Error curves of the deep models are smoother than that of **SVR**, thanks to temporal coherency imposed by recurrent networks.

References

[1] V. Blanz, C. Basso, T. Poggio, and T. Vetter. Reanimating faces in images and video. In *SIGGAPH*, pages 187–194, 1999.

[2] V. Blanz and T. Vetter. A morphable model for the synthesis of 3d faces. In *Eurographics*, pages 641–650, 2003.

[3] C. Bregler, M. Covell, and M. Slaney. Video rewrite: driving visual speech with audio. In *SIGGRAPH*, pages 353–360, 2007.

[4] C. Busso, Z. Deng, S. Yildirim, M. Bulut, C. Lee, A. Kazemzadeh, S. Lee, U. Neumann, and S. Narayanan. Analysis of emotion recognition using facial expressions, speech and multimodal information. In *Sixth International Conference on Multimodal Interfaces ICMI 2004*, pages 205–211, State College, PA, October 2004. ACM Press.

[5] C. Busso and S. Narayanan. Interplay between linguistic and affective goals in facial expression during emotional utterances. In *7th International Seminar on Speech Production (ISSP 2006)*, pages 549–556, Ubatuba-SP, Brazil, December 2006.

[6] C. Busso and S. Narayanan. Joint analysis of the emotional fingerprint in the face and speech: A single subject study. In *International Workshop on Multimedia Signal Processing (MMSP 2007)*, pages 43–47, Chania, Crete, Greece, October 2007.

[7] C. Cao, Y. Weng, S. Zhou, Y. Tong, and K. Zhou. FaceWarehouse: A 3D Facial Expression Database for Visual Computing. *IEEE Transactions on Visualization and Computer Graphics*, 20(3):413–425, March 2014.

[8] Y. Cao, W. C. Tien, P. Faloutsos, and F. Pighin. Expressive speech-driven facial animation. *ACM Transactions on Graphics*, 24(4):1283–1302, 2005.

[9] E. Cosatto, J. Ostermann, H. P. Graf, and J. Schroeter. Lifelike talking faces for interactive services. *Proc IEEE*, 91(9):1406–1429, 2003.

[10] C. Ding, L. Xie, and P. Zhu. Head motion synthesis from speech using deep neural network. *Multimed Tools Appl*, 74:9871–9888, 2015.

[11] H. Ducker, C. J. C. Burges, L. Kaufman, A. Smola, and V. Vapnik. Support vector regression machines. In *NIPS*, volume 9, pages 155–161, 1996.

[12] T. Ezzat, G. Geiger, and T. Poggio. Trainable videorealistic speech animatio. In *SIGGRAPH*, pages 388–397, 2002.

[13] B. Fan, L. Xie, S. Yang, L. Wang, and F. K. Soong. A deep bidirectional lstm approach for video-realistic talking head. *Multimed Tools Appl*, 75:5287–5309, 2016.

[14] S. Hochreiter. The vanishing gradient problem during learning recurrent neural nets and problem solutions. *Int J Uncertain Fuzziness Knowl-Based Syst*, 6(2):107–116, 1998.

[15] S. Hochreiter and J. Scmidhuber. Long short-term memory. *Neural Comput*, 9(8):1735–1780, 1997.

[16] S. R. Livingstone, K. Peck, and F. A. Russo. Ravdess: The ryerson audio-visual database of emotional speech and song. In *22nd Annual Meeting of the Canadian Society for Brain, Behaviour and Cognitive Science (CSBBCS)*, 2012.

[17] S. Mariooryad and C. Busso. Factorizing speaker, lexical and emotional variabilities observed in facial expressions. In *IEEE International Conference on Image Processing (ICIP 2012)*, pages 2605–2608, Orlando, FL, USA, September-October 2012.

[18] S. Mariooryad and C. Busso. Facial expression recognition in the presence of speech using blind lexical compensation. *IEEE Transactions on Affective Computing*, 7(4):346–359, October-December 2016.

[19] H. X. Pham and V. Pavlovic. Robust real-time 3d face tracking from rgbd videos under extreme pose, depth, and expression variations. In *3DV*, 2016.

[20] H. X. Pham, V. Pavlovic, J. Cai, and T. jen Cham. Robust real-time performance-driven 3d face tracking. In *ICPR*, 2016.

[21] Y. Qian, Y. Fan, and F. K. Soong. On the training aspects of deep neural network (dnn) for parametric tts synthesis. In *ICASSP*, pages 3829–3833, 2014.

[22] S. Sako, K. Tokuda, T. Masuko, T. Kobayashi, and T. Kitamura. Hmm-based text-to-audio-visual speech synthesis. In *ICSLP*, pages 25–28, 2000.

[23] G. Salvi, J. Beskow, S. Moubayed, and B. Granstrom. Synface: speech-driven facial animation for virtual speech-reading support. *URASIP journal on Audio, speech, and music processing*, 2009.

[24] A. Wang, M. Emmi, and P. Faloutsos. Assembling an expressive facial animation system. *ACM SIGGRAPH Video Game Symposium (Sandbox)*, pages 21–26, 2007.

[25] L. Wang, X. Q. abd W. Han, and F. K. Soong. Synthesizing photo-real talking head via trajectoryguided sample selection. In *Interspeech*, pages 446–449, 2010.

[26] L. Wang, X. Qian, F. K. Soong, and Q. Huo. Text driven 3d photo-realistic talking head. In *Interspeech*, pages 3307–3310, 2011.

[27] R. J. Williams and D. Zipser. A learning algorithm for continually running fully recurrent neural networks. *Neural Comput*, 1(2):270–280, 1997.

[28] Z. Wu, S. Zhang, L. Cai, and H. Meng. Real-time synthesis of chinese visual speech and facial expressions using mpeg-4 fap features in a three-dimensional avatar. In *Interspeech*, pages 1802–1805, 2006.

[29] L. Xie and Z. Liu. Realistic mouth-synching for speech-driven talking face using articulatory modeling. *IEEE Trans Multimed*, 9(23):500–510, 2007.

[30] H. Zen, A. Senior, and M. Schuster. Statistical parametric speech synthesis using deep neural networks. In *ICASSP*, pages 7962–7966, 2013.

[31] X. Zhang, L. Wang, G. Li, F. Seide, and F. K. Soong. A new language independent, photo realistic talking head driven by voice only. In *Interspeech*, 2013.